

Mass-imbalanced fermionic mixture in a harmonic trap

B. Bazak¹

¹*IPNO, CNRS/IN2P3, Univ. Paris-Sud, Université Paris-Saclay, F-91406, Orsay, France*

(Dated: October 6, 2018)

The mass-imbalanced fermionic mixture is studied, where $N \leq 5$ identical fermions interact resonantly with an impurity, a distinguishable atom. The shell structure is explored, and the physics of a dynamic light-impurity is shown to be different from that of the static heavy-impurity case. The energies in a harmonic trap at unitarity are calculated and extrapolated to the zero-range limit. In doing so, the scale factor of the ground state, as well as of a few excited states, is calculated. In the $2 \leq N \leq 4$ systems, pure $(N + 1)$ Efimov states exist for large enough mass ratio. However, no sign for a six-body Efimov state in the $(5 + 1)$ system is found in the mass ratio explored, $M/m \leq 12$.

I. INTRODUCTION

The system of N identical fermions interacting resonantly with a distinguishable atom exhibits a rich and interesting physics, including universal phenomena and the celebrated Efimov physics. For a recent review see, e.g., Ref. [1].

An important parameter here is the ratio of the impurity mass m and the identical fermions mass M . In the ultracold limit the interaction between identical fermions can be neglected, and therefore in the heavy impurity case $m \gg M$ the problem is decoupled to N independent fermions interacting with a static impurity. The opposite limit, where $m \ll M$, corresponds to a dynamic impurity which induces interaction between the identical fermions.

The simplest non trivial example is the $(2 + 1)$ system, composed of two identical fermions of mass M and a distinguishable atom of mass m , where different particles have zero-range resonant interaction while identical particles do not interact. Efimov has shown that when the mass ratio $\alpha = M/m$ is larger than the critical value $\alpha_c = 13.607$, an infinite tower of trimers with angular momentum and parity $L^\pi = 1^-$ is produced [2]. The n -th trimer energy is $E_n = E_0 e^{-2\pi n/|s|}$, where E_0 is the trimer ground-state energy. The scale factor $s = s(\alpha)$ is a function of the mass ratio and vanishes at the Efimov threshold $s(\alpha_c) = 0$.

In the non-Efimovian regime $\alpha < \alpha_c$ the scale factor characterizes the short-distance (and large momenta) behavior of a universal trimer, which exists for $8.173 < \alpha < \alpha_c$ for finite positive scattering length [3].

The physical interpretation of the scale factor can be understood from the adiabatic hyperspherical formalism [4]. To see that, one rearranges the relative coordinates into the hyperradius ρ , the only coordinate with a dimension of length, and $3N - 1$ hyperangles. Here $\rho \propto \sqrt{mr^2 + M \sum_{i=1}^N R_i^2}$, where \mathbf{r} (\mathbf{R}_i) is the position of the distinguishable (identical) atom in the center-of-mass frame. At small ρ , where E and $1/a$ can be neglected, the hyperradial motion separates from hyperangular degrees

of freedom and is governed by

$$\left[-\frac{\partial^2}{\partial \rho^2} - \frac{3N-1}{\rho} \frac{\partial}{\partial \rho} + \frac{s^2 - (3N/2 - 1)^2}{\rho^2} \right] \Psi(\rho) = 0, \quad (1)$$

where s^2 is the hyperangular eigenvalue. The general solution of Eq. (1) is a linear combination of $\Psi_+(\rho) \propto \rho^{-3N/2+1+s}$ and $\Psi_-(\rho) \propto \rho^{-3N/2+1-s}$. The case $s^2 < 0$ ($s = is_0$) corresponds to the Efimovian regime, where this linear combination is an oscillating function, and a three-body parameter is required to fix the relative phase of Ψ_+ and Ψ_- . The non-Efimovian regime appears for $s^2 > 0$ ($s > 0$) where, far from few-body resonances, $\Psi(\rho)$ is dominated by $\Psi_+(\rho)$.

Interestingly, the same factor determines the energy of the trapped system at unitarity [5, 6], namely,

$$E = \hbar\omega(s + 2n + 1), \quad (2)$$

where ω is the trapping frequency, taken to be identical for all particles, n is a non-negative integer and the center-of-mass zero-point energy is omitted. This is because the trapping potential is involved only in the hyper-radial equation, while s is determined by the hyperangular equation which is identical in free space and in a trap. For a recent review of the trapped few-body problem, see Ref. [7].

Following Efimov, the mass-imbalanced $(2+1)$ system has attracted wide attention (see, e.g., Refs. [2, 3, 8–21]). The scale factor of the $(2+1)$ system was first calculated for the equal-mass case to be $s(1) = 1.7727$ for the 1^- ground state and $s(1) = 2.1662$ for the 0^+ excited state [10]. Later, the method was generalized to include any angular momentum and mass ratio [13]. The 1^- trimer energy crosses the dimer+atom energy in a trap at $\alpha = 8.6186$ [9]. An ultracold mixture of ${}^6\text{Li}$ and ${}^{40}\text{K}$ ($\alpha \approx 6.4$) was realized experimentally, and a strong atom-dimer attraction was observed. This attraction was interpreted as p -wave interaction between two heavy particles induced by the light atom [22].

The trend of moving from a non-Efimovian universal state to an Efimovian state with the same symmetry as the mass ratio increases was discovered also in the $(3+1)$ and $(4+1)$ systems [23–25].

The mass-imbalanced $(3+1)$ system has been the subject of a few studies [21, 23–26]. Here a tower of 1^+

Table I: The ground-state properties of mass-imbalanced ($N+1$) fermionic mixtures, for $N \leq 5$. Shown are the angular momentum and parity of the state, the mass ratio where it crosses the threshold of the system with one particle less in free space and in a harmonic trap, and the mass ratio where Efimov physics emerges. See text for references.

System	L^π	Free crossing	Trap crossing	Efimov
2+1	1^-	8.173	8.619	13.607
3+1	1^+	8.862	8.918	13.384
4+1	0^-	9.672	9.41	13.279
5+1	0^-			

Efimovian tetramers exists above $\alpha_c = 13.384$ [23], and a universal non-Efimovian 1^+ tetramer is bound in free space for $8.862 < \alpha < \alpha_c$ [24, 25]. The scale factor of the tetramer ground state has been calculated for a few mass ratios [26], while that of excited states is known only for the equal-mass case [27]. The tetramer energy crosses the trimer+atom energy in a trap at $\alpha = 8.918$ [25].

The mass-imbalanced ($4+1$) system was studied in Refs. [25, 26]. A tower of 0^- Efimovian pentamers exists above $\alpha_c = 13.279$, while a universal 0^- pentamer is bound in free space for $9.672 < \alpha < \alpha_c$ [25]. Here the scale factor is known for equal mass [27], when the pentamer is bound in free space [25] and for few other mass ratios [26]. The pentamer energy crosses the tetramer+atom energy in a trap at $\alpha = 9.41$ [25].

The ground-state properties of the ($N+1$) systems are summarized in Table I.

Very little is known about the ($5+1$) system. A simplified model explains the similar trends in the ($2+1$), ($3+1$), and ($4+1$) systems as populating a p shell atom by atom. The ($5+1$) system, therefore, should be different, since the p shell is now full and the additional atom has to open a new shell [25]. Intriguing open questions are thus the following: is there a non-Efimovian universal bound hexamer and does the six-body Efimov effect exist?

The extrapolation toward the case of fermionic polaron, corresponding to the $N \gg 1$ case, is of special interest. As a step in this direction the shell structure of the few-body systems is studied here. In contrast to the static heavy-impurity case, it is shown that non-perturbative physics arise in the dynamic light-impurity case.

The goal of this work is to study the scale factor, or equivalently the energy in a trap, of the ($N+1$) ($N \leq 5$) fermionic mixtures few lowest states, and to identify their properties. Calculation are done for a wide range of mass ratios, from the static-impurity limit $m \gg M$ to the dynamic-impurity limit $m \ll M$.

A convenient way to describe the system is the Skorniakov and Ter-Martirosian (STM) integral equation [28, 29], which deals directly with zero-range interaction by applying the Bethe-Peierls boundary condition when

two different particles approach each other. One has to solve an integral equation in $3(N-1)$ dimensions, but utilizing the system symmetries the number of dimensions can be reduced further.

For $N = 2$, the STM equation for the scale factor is reduced to a transcendental equation which can be easily solved. For $N = 3$, it can be reduced to two dimensions, allowing the solution on a grid [23]. For $N = 4$, however, a five-dimensional equation makes a grid-based approach challenging if possible at all. A method based on a Monte-Carlo process to solve the STM equation was developed for this case in Ref. [25]. However, this method is limited to bound systems and therefore cannot be used to calculate the scale factor for all mass ratios. In addition, as a fermionic Monte-Carlo method it might suffer from a sign problem if the wave function has radial nodes.

Thus we take here another approach. We solve the Schrödinger equation for the trapped system with *finite*-range interspecies potential and then extrapolate to the zero-range limit. A similar method was applied in Refs. [26, 27].

Using this method we calculate the scale factor for $0 \leq \alpha \leq 12$ for the ground state, as well as for a few lowest excited states, of the ($N+1$) fermionic system up to $N \leq 5$. We set a simple model to understand the shell structure for the static-impurity case, and explore the effects of the dynamic impurity as the mass ratio increases.

We find that no ($5+1$) Efimov states exist for $\alpha \leq 12$. As the mass ratio increases, finite-range corrections become significant and the extrapolation to the zero-range limit cannot be trusted anymore. A further study is therefore needed to explore such states for larger mass ratios, $12 < \alpha < 13.279$.

II. METHODS

As we have explained, the zero-range limit is not directly used here; instead, a series of calculations with a finite-range potential with decreasing range is used to extrapolate the zero-range limit.

The Hamiltonian of the ($N+1$) system is

$$H = T + U + V, \quad (3)$$

where T is the internal kinetic energy and U is the confining harmonic potential. Here, V is the interspecies attractive interaction, taken of the form

$$V = -V_0 \sum_{i=1}^N \exp\left(-\frac{(\mathbf{r} - \mathbf{R}_i)^2}{2R_0^2}\right), \quad (4)$$

where $V_0 > 0$ is the potential strength and R_0 is its range. We seek the limit of $R_0 \rightarrow 0$ while V_0 is tuned to keep the two-body system at unitarity.

To solve the few-body problem, we use the stochastic variational method (SVM) [30]. The wave function is expanded in an over-complete basis of correlated Gaussians, where the basis functions are chosen in a stochastic

way utilizing the variational principle. The energies and the corresponding wave functions can be found then by solving a generalized eigenvalue problem.

The basis functions are chosen to have the necessary permutational symmetry, parity π , and angular momentum L and its projection M ,

$$\phi_{LM}^\pi(A, u; \eta) = \hat{A} e^{-\frac{1}{2}\eta^T A \eta} \theta_{LM}^\pi(u; \eta) \quad (5)$$

where $\eta \equiv \{\eta_1, \dots, \eta_N\}$ is a set of N Jacobi coordinates, \hat{A} is the appropriate anti-symmetrization operator, A is an $N \times N$ real, symmetric, and positive definite matrix, and $\theta_{LM}^\pi(u; \eta)$ is the angular part. The $N(N+1)/2$ real numbers defining A are optimized in a stochastic way such as the energy is minimized. Spin and isospin functions can be introduced but are not needed here.

The angular part is characterized by the global vector representation [31, 32]. For a natural parity $\pi = (-1)^L$ it is

$$\theta_{LM}^\pi(u; \eta) = \mathcal{Y}_{LM}(\mathbf{v}), \quad (6)$$

where \mathcal{Y}_{LM} is the regular solid harmonic and $\mathbf{v} = u^T \eta$ is a global vector, whose elements are also optimized in a stochastic way.

To get the unnatural parity $\pi = (-1)^{L+1}$ for $L > 0$ one has to couple two global vectors,

$$\theta_{LM}^\pi(u; \eta) = [\mathcal{Y}_L(\mathbf{v}_1) \otimes \mathcal{Y}_1(\mathbf{v}_2)]_{LM}, \quad (7)$$

while three global vectors are needed to get the 0^- symmetry,

$$\theta_{00}^-(u; \eta) = [[\mathcal{Y}_1(\mathbf{v}_1) \otimes \mathcal{Y}_1(\mathbf{v}_2)]_1 \otimes \mathcal{Y}_1(\mathbf{v}_3)]_{00}. \quad (8)$$

The overlap of such basis functions, as well as the matrix elements of the Hamiltonian, are known analytically [27, 30–33].

For a given number of particles, angular momentum, and parity, the ground-state energy is calculated for various potential ranges. From these energies, the zero-range limit is extrapolated.

Typical results for the $(2+1) 1^-$ ground state are shown in Fig. 1, where results calculated from finite-range potentials are compared to the zero-range results. The radius of convergence for the extrapolation is shown to be much larger for $\alpha = 4$ than for $\alpha = 12$. In the latter case, close to the Efimovian limit, the extrapolated value will be completely off if one uses, say, results with $R_0 > 0.03\sqrt{\hbar^2/m\omega}$ [26].

To estimate the extrapolation uncertainty, we fit the results with a few shortest R_0 with linear and parabolic curves and account for their differences. The error due to the finite basis set becomes significant for $N > 3$ and is also considered.

Taking the potential range to be smaller, the numerical calculation becomes harder. Therefore close to the Efimovian limit, where finite-range corrections become significant, the extrapolations can not be trusted anymore. To correctly treat this region one should use a

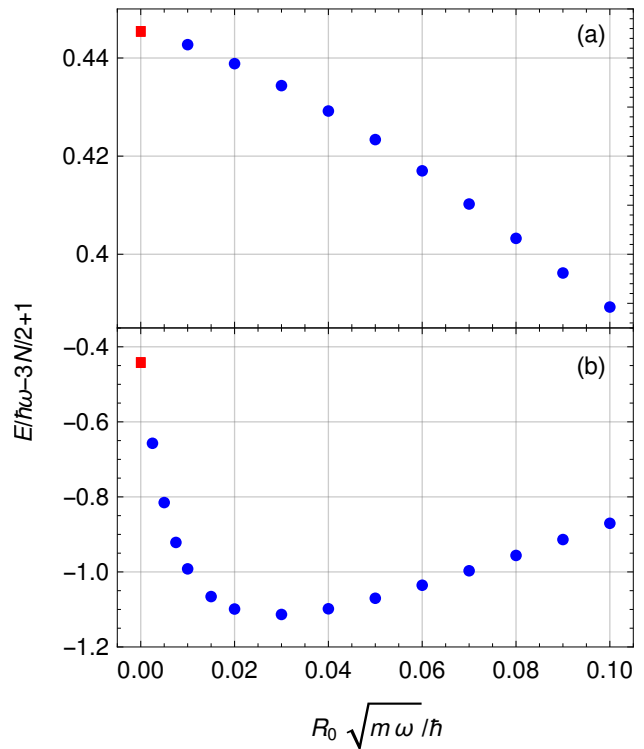


Figure 1: Convergence of finite-range potentials toward the zero-range limit $R_0 \rightarrow 0$ for the $(2+1)$ ground state. (a) $\alpha = 4$, away from the Efimovian limit. (b) $\alpha = 12$, near the Efimovian limit. The zero-range result (red square) is the exact solution of Eq. (11).

method dealing with the zero-range limit directly. For example, one would like to solve the STM equation using a diffusion Monte-Carlo (DMC)-like approach [25]. This task is left for future work.

III. RESULTS

A. The $\alpha = 0$ limit

We start to analyze the $\alpha = 0$ limit, where the impurity is infinitely heavy and therefore static. This case reduces to the problem of N trapped fermions scattering on a zero-range potential at the trap center. The analytic solution for the two-body problem is known [34], giving at unitarity an energy shift of $-\hbar\omega$ for the s shell with respect to the non interacting case. The quantum numbers characterizing a shell are the radial number n and the angular momentum l and its projection; its energy is given by

$$E_{nl} = \hbar\omega(2n + l - \delta_{l,0} + 3/2), \quad (9)$$

and the energy of the $(N+1)$ system is just a sum of N single-particle energies. To ease comparison between

Table II: The ground-state properties in the static-impurity limit, $\alpha = 0$. Shown are the energy, the angular momentum, the parity, and the shell configuration for the $(N+1)$ mixtures.

System	ϵ	π	L	Configuration
1+1	0	+	0	$0s$
2+1	1	+	0	$0s\ 1s$
		-	1	$0s\ 0p$
3+1	2	+	1	$0s\ 0p^2$
		-	1	$0s\ 1s\ 0p$
4+1	3	+	1	$0s\ 1s\ 0p^2$
		-	0	$0s\ 0p^3$
5+1	4	-	0	$0s\ 1s\ 0p^3$

clusters with different particle numbers, the zero-point energy $\hbar\omega\ 3N/2$ is subtracted. Energy is measured in units of $\hbar\omega$ and with respect to the dimer energy, i.e.

$$\epsilon = E/\hbar\omega - 3N/2 + 1. \quad (10)$$

Only interacting states, i.e., those states which have an atom in an s shell, are considered.

Applying the fermionic symmetry, the spectrum and properties of the $(N+1)$ systems can be calculated. Table II summarizes the ground-state properties of the $(N+1)$ systems. For completeness, the properties of the two lowest excited states are also tabulated in the Appendix. Here and thereafter we ignore the trivial $2L+1$ degeneracy due to different total angular momentum projections.

B. The (2+1) case

We move now to the general mass-imbalanced case and start with two identical fermions interacting with a distinguishable atom.

For the natural parity case, the scale factor s corresponding to a total angular momentum L is the solution of a transcendental equation,

$$\frac{2}{\Gamma(a-1/2)\Gamma(b-1/2)} + \frac{(-\gamma)^L}{\sqrt{\pi}\Gamma(c)} {}_2F_1(a, b; c; \gamma^2) = 0 \quad (11)$$

where $a = 1 + (L-s)/2$, $b = 1 + (L+s)/2$, $c = L + 3/2$, ${}_2F_1$ is the hypergeometric function, and $\gamma = \alpha/(\alpha+1)$ [13].

Unnatural parity means here that both identical fermions are excited to $l > 0$ shell, resulting in a non interacting case that will be ignored here.

For $\alpha = 0$ the ground state has two degenerate states, 1^- and 0^+ , where in the first case the additional atom populates a p shell while in the latter it sits in an excited s shell. The energy degeneracy is lifted for $\alpha > 0$,

where the dynamic impurity induces interaction between the identical fermions, which is attractive (repulsive) for an odd (even) angular momentum. Hence, the 1^- state becomes the ground state.

This behavior can be understood in the Born-Oppenheimer (BO) approximation, which holds for $\alpha \gg 1$ [8]. Utilizing the mass difference, the distance between heavy particles $\mathbf{R} = \mathbf{R}_1 - \mathbf{R}_2$ can be treated as a parameter in the light-particle equation, which becomes simply the double-well potential problem, with the known eigenvalues $\epsilon_{\pm}(R)$. In the heavy-particle equation, $\epsilon_{\pm}(R)$ has the meaning of an effective potential and is attractive or repulsive, depending on the parity. Applying the fermionic symmetry for heavy particles' permutation, the effective potential for odd- L states is found to be attractive and goes like $-1/mR^2$ for $R \ll a$, while the effective potential for even- L states is repulsive.

For the attractive channel, the mass ratio governs the competition between the centrifugal barrier $\propto L(L+1)/MR^2$ and the effective attraction. Increasing α tips the scales in favor of the attraction; hence the trimer energy decreases. In a trap the trimer energy crosses the dimer+atom energy ($\epsilon = 0$ in our conventions) for α slightly larger than needed in free space. Increasing α further the effective interaction becomes purely attractive and the system becomes Efimovian. In the $(2+1)$ system, the 1^- symmetry is the only symmetry where this phenomenon occurs.

To benchmark our method, we calculate the unitary $(2+1)$ trapped system energy by extrapolating finite-range results to the zero-range limit. The scale factor can be easily calculated from Eq. (11) and is connected to the energy in a trap by Eq. (2), giving here (for $n = 0$) $s = \epsilon + 1$. Hence, the Efimovian limit $s = 0$ corresponds here to $\epsilon = -1$. Our results are plotted in Fig. 2, showing a nice agreement with the solutions of Eq. (11). The limit of $\alpha = 0$ from Tables II, VII and VIII is also reproduced.

Note that in a trap, each solution of Eq. (11) starts a ladder of solutions, corresponding to hyperradial excitations and giving an additional $2\hbar\omega$ for each hyperradial node. The first excited state of the 1^- symmetry is also shown in Fig. 2.

C. The (3+1) case

We now add another identical particle and move to the $(3+1)$ system. For $\alpha = 0$, the ground state has two degenerate states, 1^+ and 1^- , both with $\epsilon = 2$. These states have different atomic configurations: while in the 1^+ state the additional atom sits in a p shell, the 1^- state corresponds to atom-trimer s -wave scattering. d -wave atom-trimer scattering states, corresponding to 1^- , 2^- , and 3^- symmetries, have higher energy in this limit, $\epsilon = 3$.

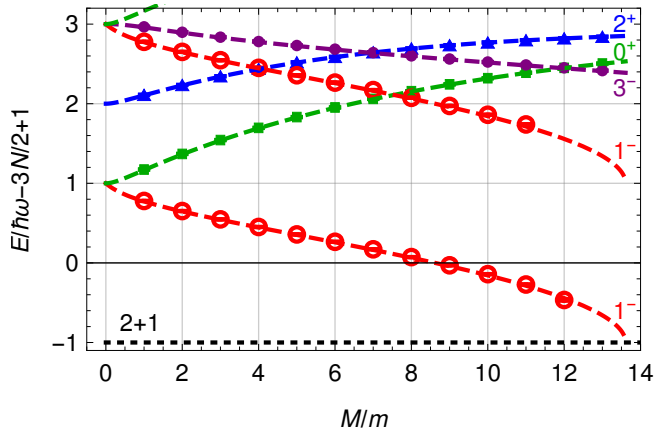


Figure 2: The energy of the unitary (2 + 1) trapped system is shown as a function of the mass ratio for a few lowest states. Symbols are the zero-range extrapolation from finite-range potentials, and dashed curves are the zero-range results calculated from Eq. (11). The Efimovian limit $s = 0$ is the dotted horizontal line, which the lowest 1^- curve hits at $M/m = 13.607$.

The energy degeneracy is lifted for $\alpha > 0$, where the 1^+ state energy becomes lower than the 1^- state energy, in qualitative agreement with the BO picture where the interaction induced by the impurity is attractive in a p wave and repulsive in an s wave.

For a larger mass ratio, the 1^+ state becomes bound in free space, then crosses the trimer+atom threshold in a trap, and eventually reaches the Efimov threshold, corresponding here to $\epsilon = -2.5$. States of other symmetries, nevertheless, does not reach the Efimov limit for any mass ratio smaller than the (2 + 1) Efimov threshold [23].

The 1^+ ground-state scale factor has been calculated in Ref. [25] using a grid-based method, similar to that of Ref. [23]. That method is more accurate than our current method and can be used up to, and even beyond, the Efimov limit. For a benchmark, we compare in Fig. 3 the results of both methods, which are in nice agreement. The $\alpha = 0$ limit from Table II is also reproduced. For this symmetry the calculations for $\alpha > 10$ become sensitive, signing a non universal resonance, identified in Ref. [26] to occur at $\alpha = 10.4(2)$ for a Gaussian interaction.

The scale factor of the 1^- lowest excited state has been calculated for an equal-mass system only [27]. Our results are tabulated in Table III and shown in Fig. 3, agreeing well with the $\alpha = 0$ limit and with the $\alpha = 1$ result of Ref. [27].

The bending in the 1^- energy around $\alpha = 2$ is to be understood as level repulsion with an excited 1^- state. To make this point clear, the energies of a few lowest 1^- states are shown in Fig. 4. The atomic configurations for $\alpha = 0$ are the following. The state with $\epsilon = 2$ corresponds to the configuration $0s0p1s$, i.e. an atom-trimer s -wave state, while for $\epsilon = 3$ it is $0s0p0d$, i.e. an atom-trimer d -wave state. A clear avoided crossing between these states

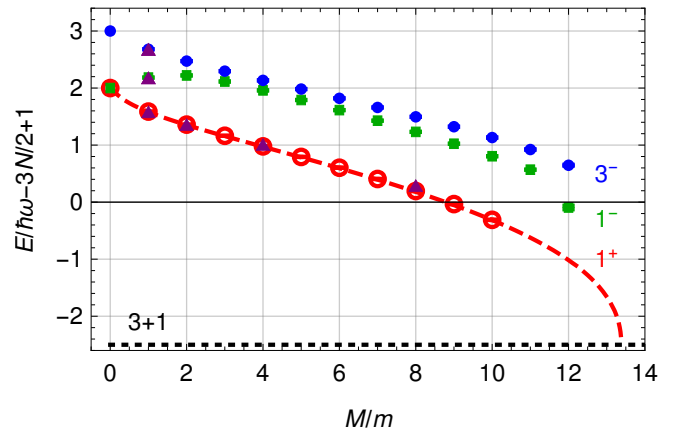


Figure 3: The energy of the unitary (3+1) trapped system is shown as a function of the mass ratio for a few lowest states. Symbols are the zero-range extrapolation from finite-range potentials, and the dashed curve is the zero-range result of Ref. [25]. The results of Refs. [26, 27] are shown as purple triangles. The Efimovian limit $s = 0$ is the dotted horizontal line, which the 1^+ curve approaches at $M/m = 13.384$.

Table III: The energies of the trapped tetramer lowest 1^- state.

M/m	This work	Ref. [27]	M/m	This work
0	2		6	1.613(1)
1	2.183(2)	2.177(4)	7	1.428(1)
2	2.221(2)		8	1.232(1)
3	2.115(2)		9	1.024(1)
4	1.959(1)		10	0.805(2)
5	1.791(1)		11	0.569(3)

is seen around $\alpha = 2$.

Note, however, that the crossing of levels with different quantum numbers is allowed. States with different hyperradial quantum number n can therefore cross, and are also shown in Fig. 4.

The next state, with 3^- symmetry, is also shown in Fig. 3. It moves closer to the 1^- state as the mass ratio increases. Since the lowest 1^- for large α is dominated by a d -wave atom-trimer state, like the 3^- state, this similarity makes sense. As we show later, this phenomena also exists, and is even stronger, for larger N .

D. The (4+1) case

Adding another identical particle, we now consider the (4 + 1) system.

For $\alpha = 0$, two states are degenerate at $\epsilon = 3$, with symmetries 0^- and 1^+ . In the 0^- state the additional atom populates the last place in the p shell, while the 1^+ state corresponds to atom-tetramer s -wave scattering.

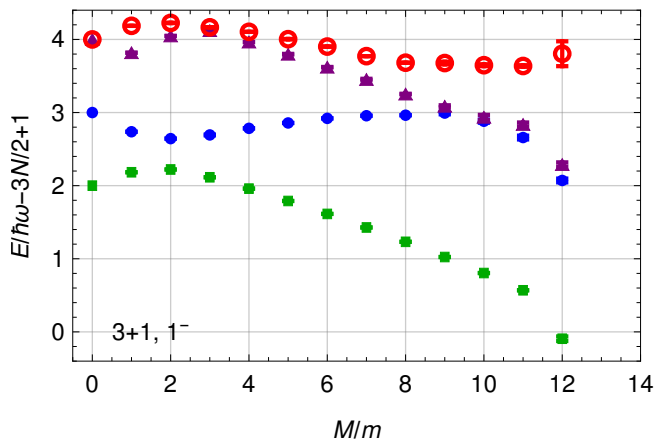


Figure 4: The energy of the unitary (3+1) trapped system is shown as a function of the mass ratio, for a few lowest 1^- states.

Table IV: The energies of the trapped pentamer 0^- state for various mass ratios.

M/m	This work	Ref. [26]	M/m	This work	Ref. [25]
0	3		6	1.01(1)	
1	2.42(1)	2.45	7	0.77(1)	
2	2.11(1)	2.15	8	0.44(1)	
3	1.83(1)		9	0.26(3)	
4	1.57(1)	1.68	10	-0.2(1)	-0.41(1)
5	1.28(1)		11	-0.5(1)	-0.90(1)

The degeneracy is lifted for $\alpha > 0$, where the 0^- state energy becomes lower than the 1^+ energy. For larger mass ratios, the 0^- state crosses the tetramer+atom energy in a trap, becomes bound in free space, and eventually reaches the Efimov threshold, corresponding here to $\epsilon = -4$ [25].

The 0^- scale factor has been calculated for a few mass ratios using finite-range models [26]. For $\alpha > 9.672$, when the pentamer is bound in free space, it was calculated by fitting the wave-function high-momentum tail to $F(Q) \propto Q^{-3N/2+1-s}$, where Q is the hypermomentum conjugate to the the hyperradius ρ and F is the momentum-space wave-function calculated in the STM-DMC method [25]. Our results are tabulated in Table IV and shown in Fig. 5.

The 1^+ scale factor has been calculated only for the equal-mass case [27]. Our results are tabulated in Table V and shown in Fig. 5. Since for large mass ratio the zero-range extrapolation is not conclusive, we cannot work close to the Efimov threshold. However, no sign for an Efimov state with any symmetry other than 0^- is found in the explored mass ratios.

Similar to the (3+1) case, the bending in the 1^+ energy results from avoided crossing around $\alpha = 1$ with another

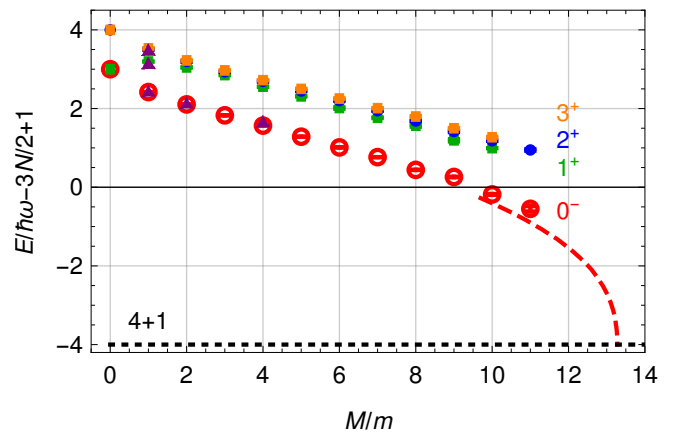


Figure 5: The energy of the unitary (4+1) trapped system is shown as a function of the mass ratio for a few lowest states. Symbols are the zero-range extrapolation from finite-range potentials, and the dashed curve is the zero-range result of Ref. [25]. The results of Refs. [26, 27] are shown as purple triangles. The Efimovian limit $s = 0$ is the dotted horizontal line, which the 0^- curve approaches at $M/m = 13.279$.

Table V: The energies of the trapped pentamer 1^+ state for various mass ratios.

M/m	This work	Ref. [27]	M/m	This work
0	3		6	2.01(2)
1	3.19(1)	3.155	7	1.77(1)
2	3.05(1)		8	1.56(3)
3	2.85(1)		9	1.19(4)
4	2.56(1)		10	0.99(1)
5	2.31(1)			

1^+ state (not shown). The latter state has $\epsilon = 4$ in the $\alpha = 0$ limit and corresponds to the d -wave atom-tetramer state. The same is true for the 2^+ and 3^+ states, also shown in Fig. 5, and indeed the energies of these state are close apart from the avoided crossing region.

E. The (5+1) case

Adding another atom, we now move to the (5+1) system. Since no room is left in the p shell, the additional atom can populate an excited s shell, keeping the 0^- symmetry of the (4+1) core, or a d shell, resulting in a 2^- state.

The energies of these states in a trap are tabulated in Table VI and plotted in Fig. 6.

As the mass ratio becomes larger, the 0^- and 2^- states becomes degenerate within our error bars.

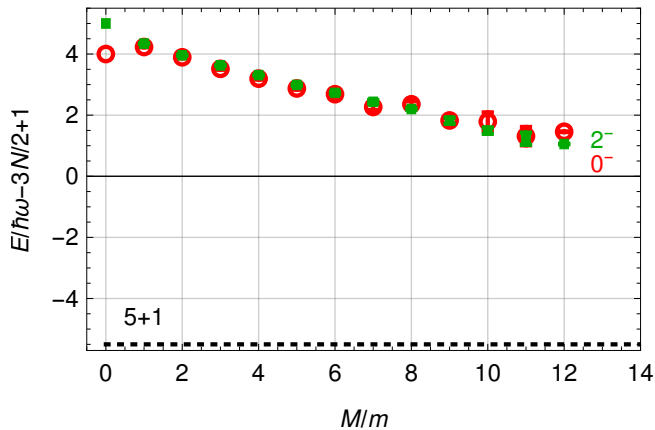


Figure 6: The energy of the unitary (5+1) trapped system is shown as a function of the mass ratio for a few lowest states. Symbols are the zero-range extrapolation from finite-range potentials. The Efimovian limit $s = 0$ is the dotted horizontal line. For the mass ratios explored here, the scale factors do not cross this limit and therefore no (5+1) Efimov effect exists.

Table VI: The energies of the two lowest (5+1) hexamer states in a trap, with 0^- and 2^- symmetries, for various mass ratios.

M/m	0^-	2^-	M/m	0^-	2^-
0	4	5	6	2.7(1)	2.73(4)
1	4.23(1)	4.34(1)	7	2.3(1)	2.44(6)
2	3.89(3)	3.96(2)	8	2.4(1)	2.20(3)
3	3.52(3)	3.63(2)	9	1.8(1)	1.8(1)
4	3.19(3)	3.31(2)	10	1.8(3)	1.5(1)
5	2.87(4)	2.99(3)	11	1.3(3)	1.2(2)

The Efimov limit corresponds here to $\epsilon = -5.5$. Our results show no sign for a (5+1) Efimov state for any symmetry up to $\alpha \leq 12$. As we have claimed, a different method would be probably needed to extend this conclusion up to the (4+1) Efimovian threshold.

IV. CONCLUSION

We study mass-imbalanced mixtures of N identical fermions interacting resonantly with a distinguishable atom. The scale factor, or the energy of the unitary system in a harmonic trap, was calculated for a few lowest

states of the $N \leq 5$ systems. We solve the trapped few-body system with finite-range inter-species potentials using the stochastic variational method. The zero-range limit is then extrapolated. The shell structure of the system is explored and the effect of level repulsion is shown, revealing the significant change from the static-impurity case to the dynamic-impurity case. A series of Efimov

Table VII: The lowest excited states properties for $\alpha = 0$. Shown are the energy, the angular momentum, the parity, and the shell configuration for the $(N+1)$ mixtures.

System	ϵ	π	L	Configuration
1+1	2	+	0	$1s$
2+1	2	+	2	$0s0d$
3+1	3	+	2	$0s1s0d$
		-	1,2,3	$0s0p0d$
4+1	4	+	1,2,3	$0s0p^20d$
		-	1,2,3	$0s1s0p0d$
5+1	5	+	1,2,3	$0s1s0p^20d$
		-	2	$0s0p^30d$

states with $N = 2, 3$, and 4 exist for large enough mass ratio. Nevertheless, no sign for the existence of a (5+1) Efimov effect is shown in the mass ratios explored here, $\alpha \leq 12$. Further studies that would deal directly with the zero-range limit should be carried out to check the validity of this statement for mass ratios up to the (4+1) Efimovian threshold.

ACKNOWLEDGMENT

I would like to thank Dmitry Petrov, Nir Barnea, Kalman Varga, Johannes Kirscher, Ronen Weiss, and Yvan Castin for useful discussions and communications. This research was supported by the Pazi Fund.

Appendix: Excited states in the $\alpha = 0$ limit

For completeness, we list here the properties of the two lowest excited states in the $\alpha = 0$ limit. The properties of the lowest-excited state are tabulated in Table VII, while those of the next-to-lowest excited state are tabulated in Table VIII.

- [1] P. Nylon and S. Endo, Efimov physics: A review, Rep. Prog. Phys. **80**, 056001 (2017).
 [2] V. N. Efimov, Energy levels of three resonantly interact-

- ing particles, Nucl. Phys. A **210**, 157 (1973).
 [3] O. I. Kartavtsev, A. V. Malykh, Low-energy three-body dynamics in binary quantum gases, J. Phys. B: At. Mol.

Table VIII: The next-to-lowest excited state properties for $\alpha = 0$. Shown are the energy, the angular momentum, the parity, and the shell configuration for the $(N + 1)$ mixtures.

System	ϵ	π	L	Configuration
1+1	4	+	0	$2s$
		+	0	$0s 2s$
2+1	3	-	1	$0s 1p$
			1	$1s 0p$
			3	$0s 0f$
			0,1,2	$0s 0p 1p$
			1,3	$0s 0d^2$
		+	2,3,4	$0s 0p 0f$
3+1	4		0	$0s 1s 2s$
			1	$1s 0p^2$
			1	$0s 1s 1p$
		-	1	$0s 2s 0p$
			3	$0s 1s 0f$
			0,1,2	$0s 1s 0p 1p$
			1	$0s 2s 0p^2$
		+	1,3	$0s 1s 0d^2$
			2,3,4	$0s 1s 0p 0f$
4+1	5		0,1,2,2,3,4	$0s 0p 0d^2$
			0,1,2	$0s 0p^2 1p$
		-	1	$0s 1s 2s 0p$
			2,3,4	$0s 0p^2 0f$
			0	$1s 0p^3$
			0,1,2,2,3,4	$0s 0p^2 0d^2$
			1	$0s 0p^3 1p$
		+	1	$0s 1s 2s 0p^2$
			3	$0s 0p^3 0f$
5+1	6		0	$0s 2s 0p^3$
			0,1,2	$0s 1s 0p^2 1p$
		-	0,1,2,2,3,4	$0s 1s 0p 0d^2$
			2,3,4	$0s 1s 0p^2 0f$

Opt. Phys. **40**, 1429 (2007).

- [4] J. Macek, Properties of autoionizing states of He, J. Phys. B: At. Mol. Phys. **1**, 831 (1968).
- [5] S. Tan, Short range scaling laws of quantum gases with contact interactions, arXiv:cond-mat/0412764 (2004).
- [6] F. Werner and Y. Castin, The unitary gas in an isotropic harmonic trap: Symmetry properties and applications, Phys. Rev. A **74**, 053604 (2006).
- [7] D. Blume, Few-body physics with ultracold atomic and molecular systems in traps, Rep. Prog. Phys. **75**, 046401 (2012).
- [8] A. C. Fonseca, E. F. Redish, and P. E. Shanley, Efimov effect in an analytically solvable model, Nucl. Phys. A **320**, 273 (1979).
- [9] D. S. Petrov, Three-body problem in Fermi gases with short-range interparticle interaction, Phys. Rev. A **67**, 010703(R) (2003).
- [10] D. S. Petrov, C. Salomon, and G. V. Shlyapnikov, Weakly Bound Dimers of Fermionic Atoms, Phys. Rev. Lett. **93**, 090404 (2004).
- [11] Y. Nishida, D. T. Son, and S. Tan, Universal Fermi Gas with Two- and Three-Body Resonances, Phys. Rev. Lett. **100**, 090405 (2008).
- [12] J. Levinsen, T. G. Tiecke, J. T. M. Walraven, and D. S. Petrov, Atom-Dimer Scattering and Long-Lived Trimers in Fermionic Mixtures, Phys. Rev. Lett. **103**, 153202 (2009).
- [13] S. T. Rittenhouse, N. P. Mehta, and C. H. Greene, Greens functions and the adiabatic hyperspherical method, Phys. Rev. A **82**, 022706 (2010).
- [14] C. J. M. Mathy, M. M. Parish, and D. A. Huse, Trimers, Molecules, and Polarons in Mass-Imbalanced Atomic Fermi Gases, Phys. Rev. Lett. **106**, 166404 (2011).
- [15] K. Helfrich and H.-W. Hammer, On the Efimov effect in higher partial waves, J. Phys. B: At., Mol. Opt. Phys. **44**, 215301 (2011).
- [16] S. Endo, P. Naidon, and M. Ueda, Universal physics of 2+1 particles with non-zero angular momentum, Few-Body Syst. **51**, 207 (2011); Crossover trimers connecting continuous and discrete scaling regimes, Phys. Rev. A **86**, 062703 (2012).
- [17] J. Levinsen and D. S. Petrov, Atom-dimer and dimer-dimer scattering in fermionic mixtures near a narrow Feshbach resonance, Eur. Phys. J. D **65**, 67 (2011).
- [18] Y. Castin and E. Tignone, Trimers in the resonant (2+1)-fermion problem on a narrow Feshbach resonance: Crossover from Efimovian to hydrogenoid spectrum, Phys. Rev. A **84**, 062704 (2011).
- [19] A. Safavi-Naini, S. T. Rittenhouse, D. Blume, and H. R. Sadeghpour, Nonuniversal bound states of two identical heavy fermions and one light particle, Phys. Rev. A **87**, 032713 (2013).
- [20] O. I. Kartavtsev and A. V. Malykh, Universal description of three two-component fermions, Europhys. Lett. **115**, 36005 (2016).
- [21] S. Endo and Y. Castin, The interaction-sensitive states of a trapped two-component ideal Fermi gas and application to the virial expansion of the unitary Fermi gas, J. Phys. A: Math. Theor. **49**, 265301 (2016).
- [22] M. Jag, M. Zaccanti, M. Cetina, R. S. Lous, F. Schreck, R. Grimm, D. S. Petrov, and J. Levinsen, Observation of a Strong Atom-Dimer Attraction in a Mass-Imbalanced Fermi-Fermi Mixture, Phys. Rev. Lett. **112**, 075302 (2014).
- [23] Y. Castin, C. Mora, and L. Pricoupenko, Four-Body Efimov Effect for Three Fermions and a Lighter Particle, Phys. Rev. Lett. **105**, 223201 (2010).
- [24] D. Blume, Universal Four-Body States in Heavy-Light Mixtures with a Positive Scattering Length, Phys. Rev. Lett. **109**, 230404 (2012).
- [25] B. Bazak and D. S. Petrov, Five-Body Efimov Effect and Universal Pentamer in Fermionic Mixtures, Phys. Rev. Lett. **118**, 083002 (2017).
- [26] D. Blume and K. M. Daily, Breakdown of Universality for Unequal-Mass Fermi Gases with Infinite Scattering Length, Phys. Rev. Lett. **105**, 170403 (2010); Few-body resonances of unequal-mass systems with infinite interspecies two-body s -wave scattering length, Phys. Rev. A **82**, 063612 (2010).
- [27] D. Rakshit, K. M. Daily, and D. Blume, Natural and un-

- natural parity states of small trapped equal-mass two-component Fermi gases at unitarity and fourth-order virial coefficient, *Phys. Rev. A* **85**, 033634 (2012).
- [28] G. V. Skorniakov and K. A. Ter-Martirosian, Three Body Problem for Short Range Forces. I. Scattering of Low Energy Neutrons by Deuterons, *Zh. Eksp. Teor. Fiz.* **31**, 775 (1956) [*Sov. Phys. JETP* **4**, 648 (1957)].
- [29] C. Mora, Y. Castin, and L. Pricoupenko, Integral equations for the four-body problem, *C. R. Phys.* **12**, 71 (2011).
- [30] Y. Suzuki and K. Varga, *Stochastic Variational Approach to Quantum-Mechanical Few-Body Problems*, (Springer, Berlin, 1998).
- [31] K. Varga and Y. Suzuki, Precise solution of few-body problems with the stochastic variational on a correlated Gaussian basis, *Phys. Rev. C* **52**, 2885 (1995).
- [32] Y. Suzuki and J. Usukura, Excited states of the positronium molecule, *Nucl. Instrum. Methods in Phys. Res., Sect. B* **171**, 67 (2000).
- [33] B. Bazak, M. Eliyahu, and U. van Kolck, Effective field theory for few-boson systems *Phys. Rev. A* **94**, 052502 (2016).
- [34] T. Busch, B. G. Englert, K. Rzazewski, and M. Wilkens, Two cold atoms in a harmonic trap, *Found. Phys.* **28**, 549 (1998).